JOURNAL OF VIROLOGY, Mar. 2006, p. 2884–2893 Vol. 80, No. 6
0022-538X/06/$08.00+0 doi:10.1128/JVI.80.6.2884–2893.2006

A Small Loop in the Capsid Protein of Moloney Murine Leukemia Virus Controls Assembly of Spherical Cores

Marcy R. Auerbach,[1,2] Kristy R. Brown,[1] Artem Kaplan,[1] Denise de Las Nueces,[1]† and Ila R. Singh[1]*

Department of Pathology, Columbia University Medical Center, 630 West 168th Street, New York, New York 10032,[1] and Integrated Program in Cellular, Molecular, and Biophysical Studies, Columbia University College of Physicians and Surgeons, New York, New York 10032[2]

Received 4 October 2005/Accepted 27 December 2005

We report the identification of a novel domain in the Gag protein of Moloney murine leukemia virus (MoLV) that is important for the formation of spherical cores. Analysis of 18 insertional mutations in the N-terminal domain of the capsid protein (CA) identified 3 that were severely defective for viral assembly and release. Transmission electron microscopy of cells producing these mutants showed assembly of Gag proteins in large, flat or dome-shaped patches at the plasma membrane. Spherical cores were not formed, and viral particles were not released. This late assembly/release block was partially rescued by wild-type virus. All three mutations localized to the small loop between α-helices 4 and 5 of CA, analogous to the cyclophilin A-binding loop of human immunodeficiency virus type 1 CA. In the X-ray structure of the hexameric form of MLV CA, this loop is located at the periphery of the hexamer. The phenotypes of mutations in this loop suggest that formation of a planar lattice of Gag is unhindered by mutations in the loop. However, the lack of progression of these planar structures to spherical ones suggests that mutations in this loop may prevent formation of pentamers or of stable pentamer-hexamer interactions, which are essential for the formation of a closed, spherical core. This region in CA, focused to a few residues of a small loop, may offer a novel therapeutic target for retroviral diseases.

Retroviral assembly is remarkable among enveloped viruses. A single viral gene product, the Gag protein, is both necessary and sufficient to direct the assembly and release of virus-like particles from the host cell. During or shortly after viral release, Gag protein is cleaved by viral protease (PR) to yield three mature proteins common to all retroviruses: MA, CA, and NC. Most retroviruses contain one or more other proteins that differ in size and function in different retroviruses (13, 42). MA associates with the membrane, NC associates with the RNA genome, and CA forms a shell around the NC-RNA complex. Located in these Gag proteins are at least three elements known to participate in retroviral assembly and release. The M (membrane-binding) domain consists of a myristate moiety together with several basic residues in the N terminus of MA and targets newly synthesized Gag proteins to the plasma membrane (11, 38). The I (interaction) domain in NC allows Gag proteins to associate with each other. The L (late) domain is a small motif that varies in location and sequence in different retroviruses (e.g., PPPY in p12 of Moloney murine leukemia virus [MoMLV] and PTAPP in p6 of human immunodeficiency virus type 1 [HIV-1]) and is essential for the final pinching off of the membrane during viral release from the host cell (14). Here we describe the identification of a novel assembly region that is distinct from these well-characterized assembly and release domains and is located in the N-terminal domain (NTD) of MoMLV CA.

Retroviral CA proteins play a crucial yet incompletely understood role in core assembly and viral release. Although there is little sequence similarity between CA proteins from different retroviruses, their secondary and tertiary structures appear to be remarkably well conserved (7, 35). During assembly the CA domain is thought to mediate Gag-Gag interactions (16, 18, 28, 35, 47). The precise nature of Gag interactions in immature particles is not known. For mature particles, the CA lattice has been modeled on X-ray structures and on cryoelectron microscopy reconstruction of CA assemblies that were generated in vitro or purified from mature virions (6, 18, 31). The model suggests that six CA NTDs form a hexagonal ring, and each ring is connected to six neighboring rings by a dimer interface between two CA C-terminal domains (CTDs), thus forming a hexameric lattice. Biochemical and genetic analysis of several retroviruses (MoMLV, Rous sarcoma virus [RSV] and HIV-1) suggest that CTDs play an important role in core assembly (10, 47). For HIV-1, the NTD is important for proper core formation and early steps following entry (37, 39, 43, 44, 46). For the NTD of MoMLV, few genetic or biochemical analyses have been performed. The recent determination of the structure of hexameric MLV CA NTD at 1.9-Å resolution (35) facilitates mutational analyses, such as this one.

We recently used genetic footprinting to analyze a portion of the MoMLV *gag* gene (2). We found that a 12-amino-acid insertion anywhere in the first 77 amino acids of the N-terminal region of CA resulted in nonviable virus, suggesting that the NTD plays an essential role in MoMLV replication. This was in contrast to the C-terminal half of MA and all of p12, where over 75% of read-through insertions resulted in viable virus. We report here the analysis of 18 mutants in the NTD of CA to further understand its role in MoMLV replication. We

* Corresponding author. Mailing address: Department of Pathology, Columbia University Medical Center, 630 West 168th Street, New York, NY 10032. Phone: (212) 305-4263. Fax: (212) 305-4189. E-mail: is132@columbia.edu.

† Present address: Harvard Medical School, Boston, MA 02115.

found that three of these mutants were severely defective for core assembly and viral release. Transmission electron microscopy (TEM) of cells producing these mutants showed assembly of Gag protein in large, flat or dome-shaped patches at the plasma membrane, without the assembly of spherical cores and without particle release. These three mutations were localized to the small loop between α-helices 4 and 5 of CA located at the periphery of the CA hexamer (35). Mutant phenotypes suggest that the insertions do not hinder the formation of a stable, planar Gag lattice. The insertions may, however, prevent the formation of pentamers or their incorporation into the lattice, both of which are essential to generate the curvature necessary to convert a planar hexagonal lattice to a sphere.

MATERIALS AND METHODS

Plasmids and mutagenesis. Our mutagenesis of MoMLV *gag* has been described in detail elsewhere (2, 40). Individual clones were screened for mutations in the NTD of CA using PCR. One primer (short G, 5′-GGCCGCGTGCAG CTTTCA) complementary to a portion of the insertion and a second primer (2366L, 5′-TTTCTTCCGGGGTTTCTCGTTT) that hybridized outside the region of mutagenesis resulted in PCR products whose lengths depended upon the location of the insertion. Insertions in the NTD resulted in products of ≤650 bp; 15 such mutants were analyzed further. Three mutants in this study (see Fig. 1, below) were from a mutagenesis using TnsABC transposase (New England Biolabs) and contained 15-nucleotide insertions, TGTTTAAACANNNNN, where N represents target sequence-derived duplicated nucleotides (M. Auerbach and I. Singh, unpublished data).

Amino acid insertion sequences for the three late mutants are as follows: 1955, VKAARGRVQLSG, located between amino acids G81 and D82; 1968, ESC TRPRAAFSP, between amino acids P86 and T87; and 1970, MKAARGRVQ LSP, between P86 and T87. The insertions in mutants 1968 and 1970 were located between different nucleotides within the same codon, resulting in different sequences due to differing reading frames. Both mutants showed similar phenotypes, suggesting there was no correlation between insertion sequence and phenotype.

High levels of viral protein production are important to visualize virion production by TEM. Late CA mutants, plus two mutants that flanked this region, were cloned into pNCS, a version of pNCA that contains a simian virus 40 origin of replication, permitting high levels of viral protein expression in 293T cells (19). Experiments were performed with pNCS and pNCA to ensure that the mutant phenotype was unaffected by expression levels. Control DNAs for cotransfection experiments consisted of pcDNA (Invitrogen), pCMS-EGFP (Clontech), and salmon sperm DNA (Invitrogen).

A protease-deficient mutant, PR(-), containing the D32L change at residue 32, was produced in wild-type (WT) pNCS and in the three release-defective CA mutants by changing nucleotides GA to CT at positions 2765 and 2766, using primers 5′CGTACCTTCCTGGTACTTACTGGGGCCCAACAC and 5′GTG TTGGGCCCCAGTAAGTACCAGGAAGGTGACG (QuikChange II site-directed mutagenesis kit; Stratagene). All PR(-) clones were sequenced, and the PR(-) phenotype was confirmed by Western blotting.

Cells, transfection, and infection. 293T cells and Rat2 cells were maintained in Dulbecco's modified Eagle's medium supplemented with 10% fetal bovine serum, L-glutamine (2.2 mM), penicillin (100 U/ml), and streptomycin (100 μg/ml). 293T cells were transfected with WT or mutant proviral DNA using LipofectAMINE Plus following the manufacturer's protocol (Invitrogen). pCMS-EGFP (Clontech) was included in transfections to verify that differences in virion production reflected true differences in phenotypes rather than variations in transfection efficiencies. Supernatants were harvested 24, 48, and 72 h after transfection, spun to pellet virions, quantified using reverse transcriptase (RT) assays, and used to infect Rat2 cells (45). Infected Rat2 cells were passaged 2 to 3 days for 10 days. Virion release was monitored by RT assays.

Virus purification and Western blot analysis. Culture supernatants were collected 48 h after transfection of 293T cells with proviral DNAs and centrifuged through 20% sucrose cushions, and pellets were resuspended in TN buffer (for RT assay) or RIPA buffer (for Western blotting) (45). Details of virus purification, lysis, and Western blot analysis were as described previously (45, 54). Goat anti-CA serum (NCI serum 79S-804; gift of S. P. Goff, Columbia University), diluted 1:5,000, was used for Western blot assays. Cell lysate blots were reprobed with rat antitubulin antibody (Pierce). Amounts of Gag protein were measured using densitometry and ImageQuant (Molecular Dynamics).

Transmission electron microscopy of 293T cells transfected with proviral DNA. 293T cells plated on 35-mm dishes (Corning 430165) and transfected with proviral DNA were fixed 24 h posttransfection using 2.5% glutaraldehyde in 0.1 M Sorenson's buffer (0.1 M H_2PO_4, 0.1 M HPO_4, pH 7.2) for at least 12 h. Samples were postfixed with 1% OsO_4 in 0.1 M Sorenson's buffer for 1 h. Enblock staining using 1% tannic acid in water was followed by washing and staining with 1% uranyl acetate (23). After dehydration through an ethanol series, cells were embedded in Lx-112 (Ladd Research Industries, Inc). Sections of 60 nm were cut on an MT-7000 RMC apparatus, placed on mesh copper grids (Electron Microscope Sciences), stained with 1% uranyl acetate and 0.4% lead citrate, and examined under a JEOL JEM-1200 EXII electron microscope. Pictures were taken on an ORCA-HR digital camera (Hamamatsu), and measurements were made using the AMT Image Capture Engine.

Analysis of viral DNA synthesized in vivo. Virions used to infect Rat2 cells were treated with DNase I (Boehringer Mannheim) to remove plasmid DNA remaining from transfections (32). Low-molecular-weight DNA (25) from infected Rat2 cells was analyzed by PCR to detect reverse transcription products. The region of CA containing the insertion was amplified by the primers 1913U (5′-GAAAAACAACGGGTGCTCTTAG) and 2134L (5′-ATTGGGCCCTTG TGTTATTCCT). Products from mutant DNA were 36 bp larger and could easily be distinguished from the corresponding WT product on high-resolution agarose gels (ISC BioExpress). PCR conditions and rat mitochondrial DNA primers were as described elsewhere (2, 40).

RESULTS

Effects of insertions on particle production. Genetic footprinting analysis of MoMLV Gag proteins revealed that a 12-amino-acid insertion in the first 77 amino acids of CA resulted in nonviable virus, suggesting that this region plays an essential role in viral replication (2). We chose 18 mutants in this region for further analyses. Fifteen of the 18 selected mutants contained 12-amino-acid insertions, and the remaining three, generated from a separate mutagenesis, contained five-amino-acid insertions (Fig. 1). The insertions were distributed throughout the N-terminal region of CA (Fig. 1A): six were within the α-helices, three were in the β-hairpin at the N terminus, another three were in the loop between α-helices 4 and 5, and the remaining six were in turns between helices.

To test whether the CA mutants were affected in virion production, 293T cells were transfected with mutant proviral DNAs and virion release into the supernatant was measured by assaying for RT activity (45). Most mutants released near-WT levels of virus (RT activity, ~60 to 120% of WT), suggesting no significant block to particle release (Fig. 1B). However, three mutants, Ins1955, Ins1968, and Ins1970, (hereon called 1955, 1968, and 1970, respectively) consistently produced a 5- to 10-fold reduction in released RT activity. These three were clustered in a six-amino-acid region in the small loop between α-helices 4 and 5 (Fig. 1; see also Fig. 6, below). The insertion for 1955 was located between amino acids G81 and D82; for 1968 and 1970, the insertion was located between amino acids P86 and T87. Each of these three mutations was also recloned into the parent proviral vector to ensure that the observed phenotype was solely due to the mutation in CA. Recloned mutants gave results that were identical to the mutants initially isolated from our libraries.

The N-terminal CA mutations were noninfectious. To investigate whether the mutant particles released from cells were capable of completing the replication cycle, released particles were assayed for infectivity. Equal amounts of virions from transfections (based on RT activity) were used to infect Rat2

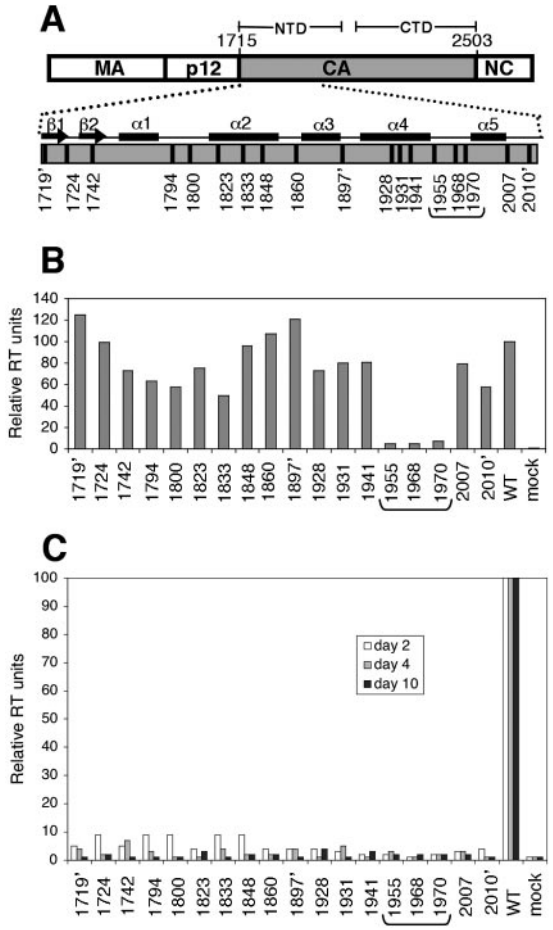

FIG. 1. Insertional mutations in NTD of MoMLV CA. (A) MoMLV Gag polyprotein. CA polypeptide (nucleotides 1715 to 2503) is highlighted in gray, with 1′ being the first nucleotide of pNCA, the infectious MoMLV clone. The positions of the β-hairpin and α-helices 1 to 5 of CA are indicated (35). Locations of mutations are denoted by vertical bars. Mutants are designated by the nucleotide position at the 5′ end of the insertional mutation. The three mutants between α-helices 4 and 5 (marked by a bracket) are the focus of this study. Three mutants generated from a separate mutagenesis contained five-amino-acid insertions and are indicated with an apostrophe in all panels. (B) Viral production assayed by RT activity in supernatants of cells transfected with proviral DNAs. RT activity of WT virus was set to 100 (average of three experiments). (C) Infectivity of mutants as measured by virus spreading assay. Culture medium from cells transfected with mutant proviral DNAs was used to inoculate naïve Rat2 cells. Virions released at days 2, 4, and 10 after infection were measured by RT activity in harvested supernatants (white, gray, and black bars, respectively).

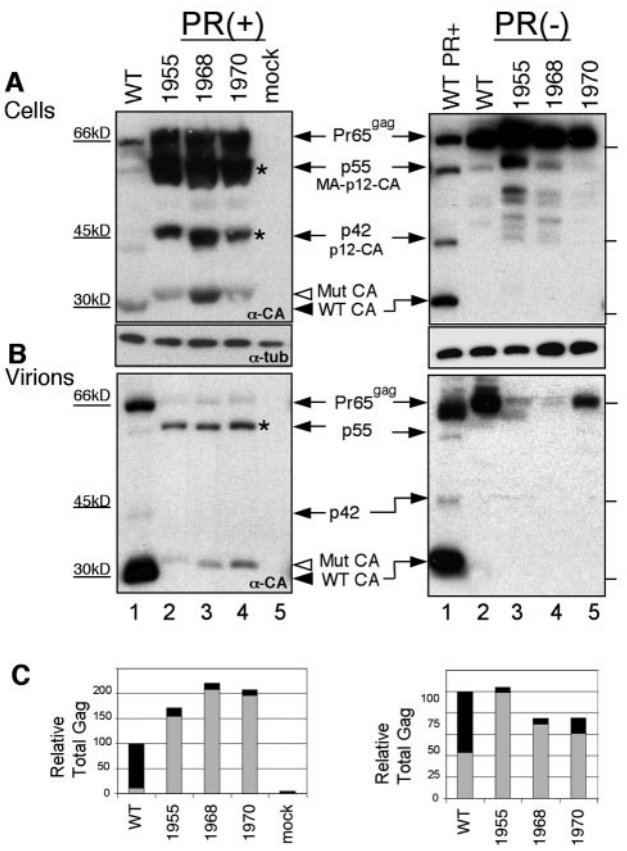

FIG. 2. Gag proteins of release-defective mutants. (A) Viral protein expression in cells transfected with proviral DNA. Western blot analysis using anti-CA polyclonal serum detected CA and other Gag intermediates 48 h after transfection. The arrow indicates the position of the Gag precursor ($Pr65^{gag}$) and intermediates. Open arrowhead, mutant CA protein; closed arrowhead, WT CA protein. Asterisks mark intermediates of Gag processing. The lower blot in panel A is the same blot and was probed with antitubulin antibody. Mutants in the context of an inactive viral protease are shown in the right panel. (B) Virions released into the medium following transfection with proviral DNA were concentrated and lysed, and the proteins were analyzed by Western blotting using anti-CA antibodies. (C) Particle release was defective for mutants 1955, 1968, and 1970. Gag proteins were quantified from blots. Gray bars represent intracellular Gag protein (from panel A, using lower exposures to ensure that signals were in the linear range for film), and black bars denote Gag released in pelleted virions (from panel B). The total amount of Gag protein in wild-type virus was set to 100%.

cells. WT virus production peaked in 2 days. In contrast, all 18 CA mutants failed to display any RT activity even after 10 days in culture (Fig. 1C). This was not surprising, since footprinting analysis shows that an insertion anywhere in the N-terminal 77 amino acids of CA results in noninfectious virus (2). In the footprinting study, functional selection for mutants was performed within 48 h of infection. By monitoring release for up to 10 days, the current study rules out delayed release phenotypes. The rest of this study focuses on the three mutants defective in viral release (1955, 1968, and 1970). Analysis of the remaining 15 NTD mutants, where viral release was relatively unaffected, will be reported separately.

Analysis of viral proteins produced by release-defective CA mutants. To determine whether the lack of virion release for the three CA mutants was due to lack of viral protein production, we examined levels of intracellular CA proteins in transfected cells. Figure 2A shows Western blots of cell lysates prepared 48 h after cells were transfected with proviral DNA. The major intracellular species of WT Gag was the $Pr65^{gag}$ precursor protein. Lesser amounts of mature CA (migrating at 30 kDa) and some intermediates of proteolytic maturation were also seen (better seen with darker exposures; not shown). The mutant CA proteins with their 12-amino-acid insertions exhibited slower mobility on sodium dodecyl sulfate-polyacrylamide gel electrophoresis gels compared to WT CA. Cells

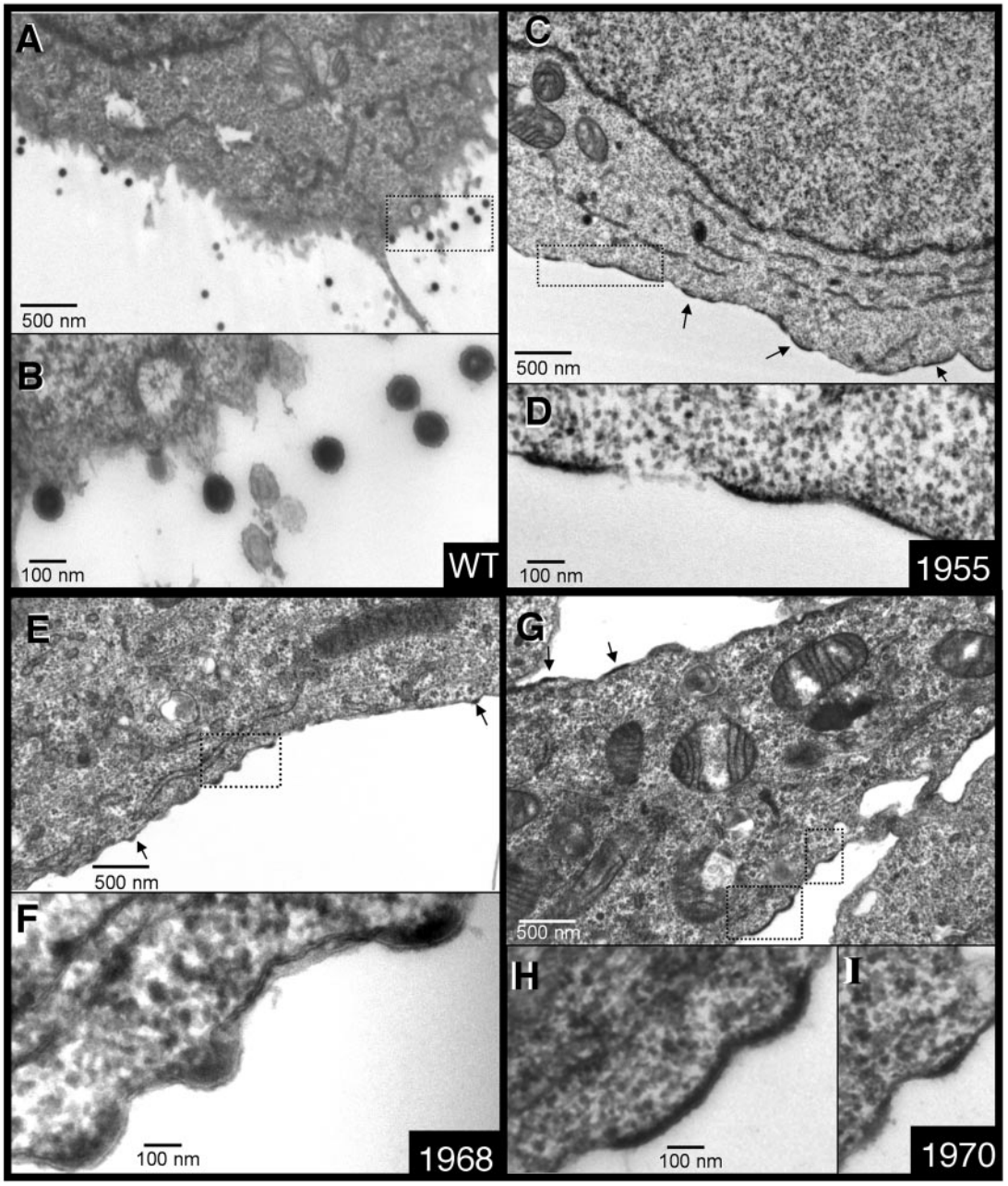

FIG. 3. TEM images of cells transfected with proviral DNA from WT and CA mutant virus: WT (A and B), 1955 (C and D), 1968 (E and F), and 1970 (G to I). Each panel shows a field at ×20,000 magnification (A, C, E, and G). Areas within fields (marked by rectangles) are magnified 75,000-fold (B, D, F, H, and I). Arrows indicate Gag assemblies beneath the plasma membrane. Scale bars are as shown.

expressing the release-defective mutants showed significantly higher amounts of $Pr65^{gag}$ precursor and processing intermediates but comparatively lower amounts of mature CA protein. In addition, the mutants produced processing intermediates barely seen with WT virus (Fig. 2A). The identity of these intermediates was inconclusively determined by probing the same blots with antibodies against MA and p12 (data not shown). Such intermediates may have very short lives in cells producing WT virus because they are incorporated into virions, which exit the cell. However, in mutants where virion release is impaired, these intermediates appear to accumulate at much higher levels. In summary, the presence of abundant amounts of Gag proteins in cells, at least some of which were normally processed, suggested there was no significant defect in the synthesis or stability of mutant CA proteins that could account for the observed defect in virion release.

We analyzed Gag proteins in the released virions by Western blot assays using an anti-CA antibody. The total amount of Gag in the supernatant was much lower for the release-defective mutants (10 to 15% of WT). The mutants contained significantly less mature CA and more unprocessed Gag intermediates compared to WT virions (Fig. 2B) or to

mutants that flank the release-defective mutants (data not shown). The Gag intermediate migrating at 55 kDa (MA-p12-CA) was present in higher amounts for the mutants. We calculated the efficiency of virion release by measuring the amount of Gag proteins released into the medium relative to amounts of intracellular Gag. Particle release for the three mutants was 10- to 20-fold less efficient than for WT (Fig. 2C). These results suggest a block for the mutants at viral assembly, release, or both.

The budding defect caused by a mutation in the HIV-1 late domain has been reported to be suppressed by inactivation of the viral protease (26). To test if a similar mechanism played a role with the CA-loop mutants, we generated protease-defective virions for each of our three mutants by replacing the active site residue (D32) of the viral protease with leucine (15). As expected for the PR(-) mutant with wild-type CA sequence [WT/PR(-)], processing of the Gag precursor into mature Gag proteins was abolished (Fig. 2A, right panel, lane 2) without interfering with the release of virions into the medium (Fig. 2B, right panel, lane 2). However, an intracellular accumulation of the Gag precursor proteins was seen with the CA mutant/PR(-), compared to WT/PR(-). Like the CA mutants in the wild-type protease background (Fig. 2B, left panel), mutants in the PR(-) background also displayed reduced levels of viral release (Fig. 2B, right panel). Overall, particle release for the three mutants in the context of PR(-) was 5- to 20-fold less efficient than for WT/PR(-) (Fig. 2C). These results demonstrate that the defect in viral release caused by insertions in the loop between α-helices 4 and 5 of CA cannot be suppressed by inactivation of the viral protease. This suggests that the block to core assembly and release is independent of Gag maturation.

TEM analysis of CA mutants. We proceeded to examine why release of mutant virions from cells was blocked, despite sufficient viral protein synthesis and processing. Indirect immunofluorescence experiments using anti-CA antibody to visualize viral protein in transfected cells with proviral DNA did not show significant differences in the intracellular localization of mutant CA protein (data not shown). We therefore used TEM to examine thin sections of cells transfected with proviral DNA (Fig. 3). The predominant viral form for the WT sample consisted of spherical particles located just outside the cell, no longer attached to the plasma membrane (Fig. 3A and B). Less common were viral structures still associated with the plasma membrane. These structures consisted of material that was of the same electron density as WT Gag protein and lined the cellular face of the plasma membrane. Though rarely seen, they appeared as small (30- to 100-nm) flat patches and dome-shaped structures (70 to 120 nm), as well as more spherical structures, most likely representing progressive stages in core assembly. These structures were never seen in nontransfected cells and could be easily distinguished from clathrin-containing structures, due to the different thickness and opposite curvatures. These viral structures were rarely seen in cells producing WT virus (10 such structures were seen upon counting 200 released particles). This was presumably because these intermediates were rapidly converted to spherical virions and released. In contrast, the viral release-defective CA mutants showed a predominance of flat patches and dome-shaped structures, with an electron density akin to WT Gag protein, localized to the plasma membrane. Unlike the rare and small structures seen with WT virus, these flat or domed structures were usually much larger for mutants 1955 and 1970 (Fig. 3C and D and G to I) and occupied large fractions of the plasma membrane. The low amount of virions produced from cells transfected with the mutants made it highly improbable that we would visualize budded virions by TEM. Indeed, released virions were never observed with these three CA mutants despite extensive analysis of several EM grids. Immature particles tethered by a stalk, as seen with L-domain mutants of many retroviruses (14), were also never seen with our CA mutants. Cells transfected with another insertional mutant (Ins1928) in the NTD showed release of spherical particles (not shown).

The electron-dense patches at the plasma membrane had a consistent and characteristic curvature for each mutant. Mutants 1955 and 1970 showed larger patches (200 to 400 nm) with less curvature (radii, 150 to 400 nm). Mutant 1968 showed smaller (100 nm) and more curved patches (radii, 100 to 120 nm). These differences may represent slightly different Gag superstructures assembled by each mutant. Thus, mutant Gag proteins assembled at the plasma membrane in large, dome-shaped patches and appeared incapable of assuming the spherical shape normally associated with MoMLV cores. Unlike intermediate stages of WT core assembly, which were rarely seen, these patches were abundant, suggesting that they might be long-lived and unable to progress to budding virions.

Complementation of CA mutants by WT CA. To gain further insight into the mechanism of block in core assembly, we performed complementation experiments (Fig. 4). WT and mutant proviral DNAs were introduced into 293T cells at different ratios. Supernatants were harvested, and RT activity was measured. When equal amounts of WT and mutant DNAs were introduced into cells, near-WT levels of virions were released into the medium, suggesting that CA protein from WT virus complemented mutant CA protein function (Fig. 4A). The RT activity from these cotransfections was associated with pellets derived from a high-speed spin and therefore likely to be virion associated. As the amount of mutant DNA in the cotransfections increased with respect to the WT (keeping total DNA constant), there was a progressive decrease in virion release (Fig. 4A). A similar decrease was seen when increasing amounts of nonviral DNA (e.g., expression plasmid for enhanced green fluorescent protein [EGFP], salmon sperm DNA, or pcDNA) were used with WT DNA in cotransfections (Fig. 4A, right panel). This decrease was therefore attributed to a progressive decrease in WT proviral DNA and not due to a dominant-negative effect of the CA mutations.

Virions released from cotransfected cells were analyzed by Western blotting. Mutant CA proteins, with their 12-amino-acid insertions, migrated slower than WT CA protein. Virions released from cotransfected cells clearly contained both WT and mutant CA proteins (Fig. 4B). Since very little mutant CA protein was seen in released virions when mutant DNA alone was used in the transfection, the presence of significant amounts of mutant CA protein in virions released from cotransfected cells was most likely due to mutant CA associating with WT CA to generate mixed particles. When at least 25% of the DNA used in the transfection was from WT DNA, viral release was efficient. When WT DNA constituted only 10%, almost no virus was released, suggesting that when the CA

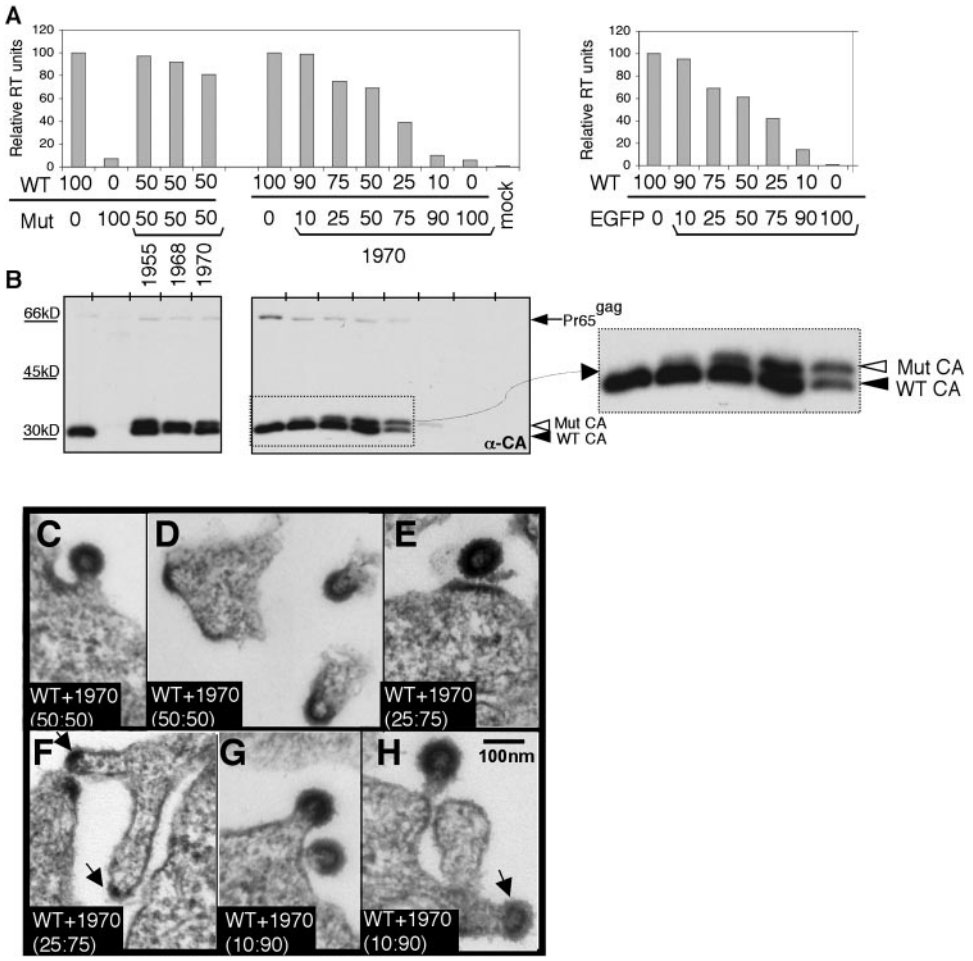

FIG. 4. WT virus can rescue CA mutants. (A) Virions released upon introduction of a mixture of WT and mutant DNA into cells. On the left, cells were cotransfected with equal amounts of WT and 1970 DNA. On the right, increasing amounts of mutant DNA were used, keeping the total DNA amounts constant. Supernatants were analyzed for RT activity 48 h posttransfection. As a control, the right panel shows increasing amounts of nonviral DNA (expression plasmid for EGFP) added to WT DNA in cotransfections. (B) Western blot of pelleted virions released from cotransfected cells using anti-CA polyclonal serum. A short exposure allows mutant and WT CA proteins (open and closed arrowheads, respectively), differing in size by 12 amino acids, to be distinguished. EM images are of 293T cells cotransfected with WT and mutant proviral genomes at different ratios, as follows: (C and D) WT and 1970, 50:50; (E and F) WT and 1970, 25:75; (G and H) WT and 1970, 10:90. Arrows indicate Gag assembly at the membrane. Bar, 100 nm.

protein population consisted mostly of mutants, rescue did not occur. As expected, WT and mutant CA proteins were present in lysates made from cotransfected cells (not shown). Cotransfection of 1955 or 1968 with WT proviral DNA at different DNA ratios showed similar results. Likewise, both WT and mutant genomes were detected when viral RNA from mixed virions was examined by RT-PCR (not shown).

TEM of cells producing both WT and mutant CA proteins. Cells cotransfected with WT and mutant proviral DNAs were examined by TEM. When equal amounts of WT and 1970 were used, virions were assembled and released at the plasma membrane (Fig. 4C and D), suggesting that WT CA rescued the mutant defect. Released particles were often incomplete spheres with a "tail" of membrane and cytoplasm (Fig. 4D). Such incomplete particles were never seen with WT CA alone. When higher amounts of mutant DNA were used, the mixed virions consisted of released particles (Fig. 4E), flat patches of Gag located at the ends of long, broad processes (Fig. 4F), and domes, spherical particles tethered by a broad-based stalk (Fig. 4G and H). Most released particles were immature, i.e., they had the characteristic "railroad track" appearance in their cores (52), though mature particles were also observed.

Early stages of infection with mixed virions. When cells were transfected with mutant proviral DNA alone, the amounts of particles released were too small to determine if the mutants were functional for early steps of viral entry and replication. We therefore turned to the particles released from cells cotransfected with mixtures of WT and mutant proviral DNAs. As shown in Fig. 4, when WT proviral DNA constituted at least 25% of the DNA used in the transfection, mostly spherical particles containing both WT and mutant CA proteins were released. To determine if these mixed virions were infectious, they were added to naïve Rat2 cells and the amount of virus released in the medium was measured by RT activity (Fig. 5A). As expected, particles resulting from WT viral DNA alone were infectious and those from the mutant alone were not.

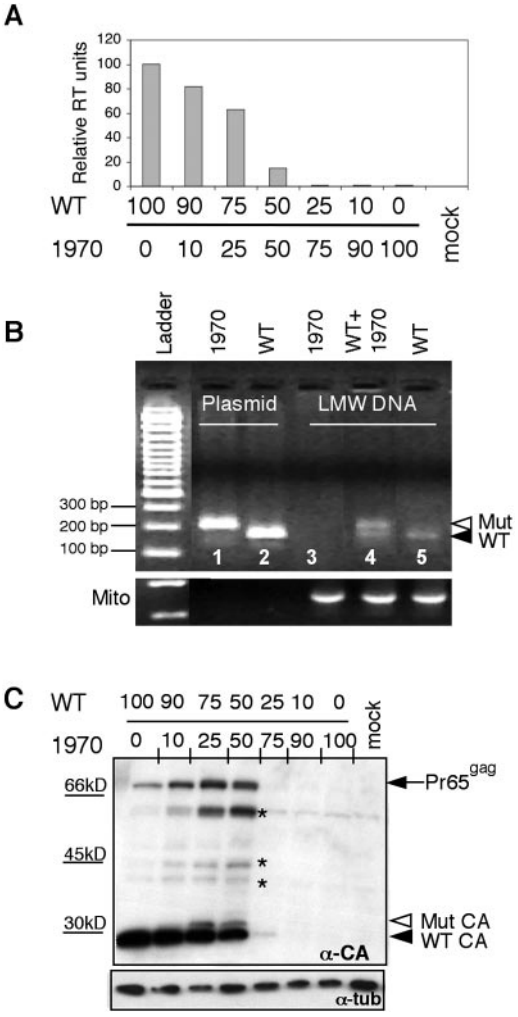

FIG. 5. Mixed virions are infectious. (A) The ability of mixed virions to infect cells was assayed using the viral spreading assay. Culture medium was collected after cotransfection with WT and mutant proviral DNAs in the indicated ratios. Equal amounts of released virus were used to inoculate naïve Rat2 cells. RT activity was measured in supernatants harvested 36 h after inoculation. (B) PCR using low-molecular-weight DNA from infected Rat2 cells. PCR primers flanked the region containing the insertional mutations, producing a 243-bp product from WT viral DNA and 279 bp from the mutant. Template DNAs consisted of mutant and WT proviral plasmid DNA (controls in lanes 1 and 2) and low-molecular-weight DNA from Rat2 cells infected with mutant virions (lane 3), mixed virions (cotransfections were done with equal amounts of WT and 1970 proviral DNA; lane 4), and WT virions (lane 5). The WT resulted in a PCR product of the expected size (lower arrow), while 1970 alone resulted in no PCR product, since it did not make virions. Mixed virions resulted in a slower-migrating band corresponding to the mutant product and a faster one for WT (doublet). PCR products resulting from amplification of rat mitochondrial DNA (bottom gel in panel B) indicated that nearly equal amounts of template were used in the analysis. (C) Rat2 cell lysates were harvested 36 h after inoculation with mixed virions and analyzed by Western blotting using anti-CA polyclonal serum. Arrows indicate WT and mutant CA protein. The same blot reprobed with antitubulin antibodies is shown below to indicate equal loading of lanes on the gel.

As the amount of mutant DNA in the cotransfections increased, the virions produced were less infectious. We next attempted to determine if only WT particles were responsible for infectivity or whether mixed virions containing mutant CA protein or mutant genome could undergo early steps of viral replication. We isolated low-molecular-weight Hirt DNA from infected cells and analyzed newly synthesized viral DNA by PCR, using primers that could distinguish WT DNA from mutant (Fig. 5B) (25). The WT sample resulted in a PCR product of the expected size, while 1970 alone resulted in no PCR product since it did not make virions. When mixed virions were used for infections (cotransfections were done with equals amounts of WT and 1970 DNA), two PCR products were observed, a slower-migrating band corresponding to the mutant product and a faster one for WT. This indicated that genomes of the 1970 mutant were packaged, released, and reverse transcribed upon entry into cells. To ensure that the PCR products were derived from reverse transcription products and not from plasmid DNA that was carried over from the transfection, viral supernatant was treated with DNase I prior to its use as inoculum. The finding that no PCR product was generated upon infection with particles released from transfection with 1970 alone further confirmed lack of carryover of plasmid DNA. We verified that 1970 genomes were being packaged into mixed virions by making RNA from pelleted virions and using RT-PCR to detect 1970 genomes (data not shown). It is likely that the CA mutations do not prevent early stages of replication and that their defect is localized to core assembly and viral release.

To confirm that the CA mutant was able to undergo stages after reverse transcription, we looked for mutant CA protein following infection. Western blot analysis of infected Rat2 cell lysates indicated that mutant CA protein was synthesized (Fig. 5C). As the amount of mutant DNA in the transfection mixture increased, the released virions produced increasing amounts of mutant protein in the cells that they infected. However, when the proportion of mutant was three times higher than WT, no viral protein was seen in infected cells, most likely because the amounts of mixed virions produced from transfected cells were insufficient to infect naïve cells (Fig. 4A). It is likely that the mutant phenotype was localized to spherical core formation and particle release and did not affect other stages of replication.

DISCUSSION

Our previous mutational analysis of Gag protein mutants showed that the NTD of the MoMLV CA protein is remarkably intolerant of insertional mutations (2). We analyzed several NTD mutants in the current study and found that most were capable of core assembly and particle release. The exceptions were three mutations localized to the small loop between α-helices 4 and 5 of CA, corresponding to the cyclophilin A-binding loop in HIV-1 (Fig. 6). Insertions in this loop resulted in large, flat or dome-shaped assemblies of Gag at the plasma membrane. Spherical cores or budding particles were absent. The phenotype was independent of proteolytic processing of Gag, suggesting that Gag maturation did not play a role in this process. However, in the presence of WT CA protein, mutant proteins were rescued and assembled into spheres, and the resulting mixed viral particles were released from cells. The observation that very few flat or dome-shaped structures were seen in this rescue experiment suggested that these structures were true intermediates of core assembly rather than dead-end

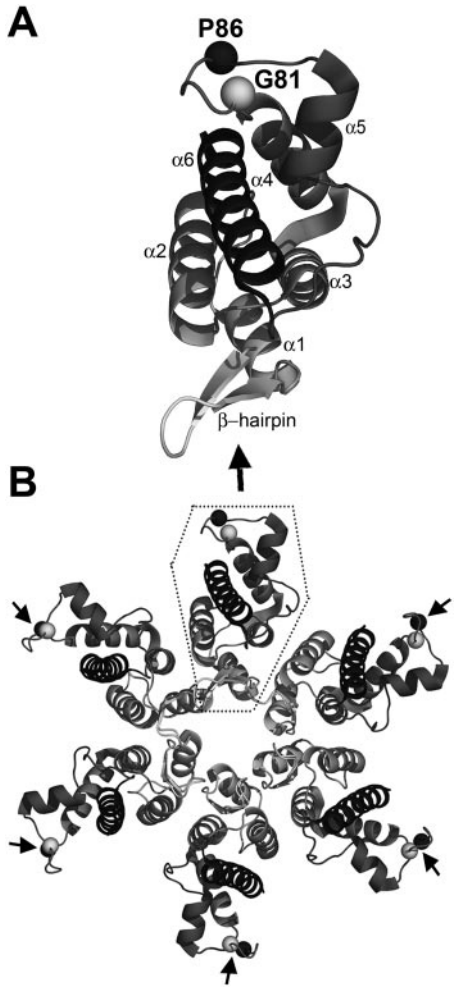

FIG. 6. Structure of the NTD of MLV CA. (A) Monomer of the NTD of MLV CA from published coordinates of the NTD hexamer. Spheres show the locations of the CA mutants in the loop between α-helices 4 and 5. Mutant 1955 is located between amino acids G81 and D82 (gray sphere); mutants 1968 and 1970 are located between P86 and T87 (black sphere). (B) Hexamer of the NTD of MLV CA (PDB, 1U7K) (28). The dotted box outlines the monomer illustrated in panel A. Drawings were made using PyMol (9).

products. Our data indicate that this loop in CA was involved in core immature particle assembly and, specifically, in formation of spherical cores.

The conclusion that a Gag assembly element exists in the NTD of MoMLV CA disagrees with some HIV-1 CA studies that have indicated the NTD may not play an essential role in particle assembly (21). For example, HIV-1 Gag proteins lacking the NTD have been shown to assemble and bud from cells (1, 3). However, a series of substitution mutations in HIV-1 CA α-helices 4 to 6 (though none were in the loop) reduced particle production (47). One mutant in α-helix 4 showed electron-dense patches of Gag beneath the plasma membrane and lacked proper curvature (47), reminiscent of our MoMLV CA mutants. We speculate that the loop and surrounding α-helices may contribute to retroviral core assembly either directly by engaging in Gag-Gag interactions required for core formation or indirectly by binding a cellular factor necessary for efficient assembly and budding.

Mature CA proteins from several retroviruses, including HIV-1 (18, 31), RSV (34), and MoMLV (17, 33, 52), form hexagonal lattices, akin to those formed by elemental carbon (20). The X-ray structure of the mature MLV CA NTD shows that NTDs assemble as hexamers, but it does not indicate how the hexamers assemble into a lattice (35). The exact time or site of hexamer assembly is not known. Since our mutants were defective for viral release, most of the Gag protein in cells expressing them was not proteolytically processed, and the lattice formed by such Gag precursors is not as well defined. It is also not clear if the protein-protein contacts formed in the immature CA lattice are retained in the mature core. However, in experiments where we rescued mutants with WT CA, we saw that the mixed virions contained mostly mature CA protein, both WT and mutant, allowing us to speculate on how such mutations might affect the hexagonal lattice structure. This is further aided by increasing evidence that immature Gag proteins also form hexagonal lattices during assembly. Electron cryomicroscopy of HIV-1 immature virions shows a hexagonal lattice (5), though unit cell dimensions of the CA hexamer in the lattice are smaller in immature virions than in mature virions (6). Also, in vitro assembly experiments utilizing MA-CA-NC domains from HIV-1 show hexameric arrangements similar to those in mature virions (27). These data suggest that factors that destabilize the hexagonal lattice in mature cores may also be applicable to immature cores. Thus, consideration of the high-resolution structure of the mature CA hexamer for mutants that do not form mature cores remains a useful method to understand the process of core assembly.

Generating curvature within a planar lattice formed by hexamers requires the incorporation of pentamers (8). A total of 12 pentamers is required to create a closed object from a hexagonal lattice. The distribution of pentamers determines the curvature and shape of the object. The MoMLV core is spherical and could be created by distributing pentamers evenly throughout the lattice. There is little structural information on retroviral CA pentamers or how they interface with hexamers. We predict that these mutations prevent hexamer-pentamer interactions or disrupt the pentamer itself, thereby blocking spherical core formation. Little is known about the mechanism of spherical lattice assembly in other cellular systems. Mutational analysis of clathrin, which forms a hexagonal lattice interspersed with pentamers around vesicles involved in membrane traffic (12), has not revealed mutants with phenotypes analogous to ours (36). These retroviral CA mutations and their corresponding lattice defects may have general relevance to other spherical protein assemblies.

An alternative possibility for lack of spherical cores that we were unable to rule out is that the insertions disrupt essential interactions between CA and other proteins (52). Such proteins could originate from the virus, e.g., MA or the cytoplasmic tail of Env, or from the host cell. For example, cyclophilin A binds the corresponding loop in HIV-1 but is not known to be involved in core formation. In support of a cellular factor binding this region, hydrogen-deuterium exchange experiments in the analogous area of HIV-1 (the cyclophilin A-binding loop and neighboring α-helices) displayed only a slight increase in hydrogen-deuterium exchange rate upon multi-

meric assembly of CA (29). This implies that the loop region does not form intramolecular protein-protein interactions, further suggesting it may bind a host factor or may be involved in intermolecular interactions (such as hexamer-hexamer or hexamer-pentamer interactions).

Host cell proteins from the multivesicular body pathway are known to participate in viral budding (14). Dominant-negative mutations in multivesicular body proteins can inhibit membrane curvature and/or viral release in the case of several retroviruses (4, 41, 48), most likely through their interaction with the viral L domain protein. A protein that promotes membrane curvature during endocytosis, endophilin 2, is known to interact with MoMLV MA (49). It is possible that a similar interaction between host cell proteins and this loop in CA might also lead to membrane curvature. Interestingly, our TEM observations of the CA mutants were reminiscent of those of the human T-cell leukemia virus type 1 late (L) domain mutants, which form curved electron-dense thickenings underneath the plasma membrane (24, 30). These L-domain mutants are likely arrested at an earlier stage of budding than L-domain mutations described for other retroviruses, including MoMLV (14, 53), HIV-1 (22), Mason-Pfizer monkey virus (51), and RSV (50). The L-domain mutants from all of these retroviruses form particles containing complete spherical cores whose release from the budding site on the plasma membrane is impaired, keeping the cores joined to the cell and to each other by narrow stalks of plasma membrane. The striking overlaps between the two phenotypes suggest a possible association between the L-domain and the NTD of CA.

In summary, we describe a novel function, i.e., the formation of spherical cores, for a domain in the NTD of MoMLV CA. This region is in the loop between α-helices 4 and 5 of CA, at the periphery of the NTD hexamer, and is essential for the progression of largely flat, multimeric Gag assembly intermediates to spheres. Since this region is localized to a small, structurally well-defined region in CA, it could serve as a potential target for antiretroviral therapy.

ACKNOWLEDGMENTS

We thank Steve Goff for numerous helpful discussions and for the anti-CA antibody. We thank Fadila Bouamr for insightful discussions at the beginning of the project. We are grateful to Sam Stampfer for generating the figure with PyMol. We thank David Sayah, Harsh Thaker, Brett Lauring, and Steve Goff for valuable comments on the manuscript.

REFERENCES

1. **Accola, M. A., B. Strack, and H. G. Gottlinger.** 2000. Efficient particle production by minimal Gag constructs which retain the carboxy-terminal domain of human immunodeficiency virus type 1 capsid-p2 and a late assembly domain. J. Virol. **74:**5395–5402.
2. **Auerbach, M. R., C. Shu, A. Kaplan, and I. R. Singh.** 2003. Functional characterization of a portion of the Moloney murine leukemia virus gag gene by genetic footprinting. Proc. Natl. Acad. Sci. USA **100:**11678–11683.
3. **Borsetti, A., A. Ohagen, and H. G. Gottlinger.** 1998. The C-terminal half of the human immunodeficiency virus type 1 Gag precursor is sufficient for efficient particle assembly. J. Virol. **72:**9313–9317.
4. **Bouamr, F., J. A. Melillo, M. Q. Wang, K. Nagashima, M. de Los Santos, A. Rein, and S. P. Goff.** 2003. PPPYVEPTAP motif is the late domain of human T-cell leukemia virus type 1 Gag and mediates its functional interaction with cellular proteins Nedd4 and Tsg101 [corrected]. J. Virol. **77:**11882–11895.
5. **Briggs, J. A., M. N. Simon, I. Gross, H. G. Krausslich, S. D. Fuller, V. M. Vogt, and M. C. Johnson.** 2004. The stoichiometry of Gag protein in HIV-1. Nat. Struct. Mol. Biol. **11:**672–675.
6. **Briggs, J. A., T. Wilk, R. Welker, H. G. Krausslich, and S. D. Fuller.** 2003. Structural organization of authentic, mature HIV-1 virions and cores. EMBO J. **22:**1707–1715.
7. **Campos-Olivas, R., J. L. Newman, and M. F. Summers.** 2000. Solution structure and dynamics of the Rous sarcoma virus capsid protein and comparison with capsid proteins of other retroviruses. J. Mol. Biol. **296:**633–649.
8. **Caspar, D. L., and A. Klug.** 1962. Physical principles in the construction of regular viruses. Cold Spring Harbor Symp. Quant. Biol. **27:**1–24.
9. **DeLano, W. L.** 2002. The PyMOL Molecular Graphics System, 0.98 ed. DeLano Scientific, San Carlos, Calif.
10. **Dorfman, T., A. Bukovsky, A. Ohagen, S. Hoglund, and H. G. Gottlinger.** 1994. Functional domains of the capsid protein of human immunodeficiency virus type 1. J. Virol. **68:**8180–8187.
11. **Facke, M., A. Janetzko, R. L. Shoeman, and H. G. Krausslich.** 1993. A large deletion in the matrix domain of the human immunodeficiency virus *gag* gene redirects virus particle assembly from the plasma membrane to the endoplasmic reticulum. J. Virol. **67:**4972–4980.
12. **Fotin, A., Y. Cheng, N. Grigorieff, T. Walz, S. C. Harrison, and T. Kirchhausen.** 2004. Structure of an auxilin-bound clathrin coat and its implications for the mechanism of uncoating. Nature **432:**649–653.
13. **Freed, E. O.** 1998. HIV-1 gag proteins: diverse functions in the virus life cycle. Virology **251:**1–15.
14. **Freed, E. O.** 2002. Viral late domains. J. Virol. **76:**4679–4687.
15. **Fu, W., and A. Rein.** 1993. Maturation of dimeric viral RNA of Moloney murine leukemia virus. J. Virol. **67:**5443–5449.
16. **Gamble, T. R., F. F. Vajdos, S. Yoo, D. K. Worthylake, M. Houseweart, W. I. Sundquist, and C. P. Hill.** 1996. Crystal structure of human cyclophilin A bound to the amino-terminal domain of HIV-1 capsid. Cell **87:**1285–1294.
17. **Ganser, B. K., A. Cheng, W. I. Sundquist, and M. Yeager.** 2003. Three-dimensional structure of the M-MuLV CA protein on a lipid monolayer: a general model for retroviral capsid assembly. EMBO J. **22:**2886–2892.
18. **Ganser, B. K., S. Li, V. Y. Klishko, J. T. Finch, and W. I. Sundquist.** 1999. Assembly and analysis of conical models for the HIV-1 core. Science **283:**80–83.
19. **Gao, G., and S. P. Goff.** 1998. Replication defect of Moloney murine leukemia virus with a mutant reverse transcriptase that can incorporate ribonucleotides and deoxyribonucleotides. J. Virol. **72:**5905–5911.
20. **Ge, M., and K. Sattler.** 1994. Observation of fullerene cones. Chem. Phys. Lett. **220:**192–196.
21. **Gottlinger, H. G.** 2001. The HIV-1 assembly machine. AIDS **15**(Suppl. 5)**:**S13–S20.
22. **Gottlinger, H. G., T. Dorfman, J. G. Sodroski, and W. A. Haseltine.** 1991. Effect of mutations affecting the p6 gag protein on human immunodeficiency virus particle release. Proc. Natl. Acad. Sci. USA **88:**3195–3199.
23. **Hayat, M. A.** 1989. Principles and techniques of electron microscopy, 3rd ed. CRC Press, Inc., Boca Raton, Fla.
24. **Heidecker, G., P. A. Lloyd, K. Fox, K. Nagashima, and D. Derse.** 2004. Late assembly motifs of human T-cell leukemia virus type 1 and their relative roles in particle release. J. Virol. **78:**6636–6648.
25. **Hirt, B.** 1967. Selective extraction of polyoma DNA from infected mouse cell cultures. J. Mol. Biol. **26:**365–369.
26. **Huang, M., J. M. Orenstein, M. A. Martin, and E. O. Freed.** 1995. $p6^{Gag}$ is required for particle production from full-length human immunodeficiency virus type 1 molecular clones expressing protease. J. Virol. **69:**6810–6818.
27. **Huseby, D., R. L. Barklis, A. Alfadhli, and E. Barklis.** 2005. Assembly of human immunodeficiency virus precursor gag proteins. J. Biol. Chem. **280:**17664–17670.
28. **Kingston, R. L., T. Fitzon-Ostendorp, E. Z. Eisenmesser, G. W. Schatz, V. M. Vogt, C. B. Post, and M. G. Rossmann.** 2000. Structure and self-association of the Rous sarcoma virus capsid protein. Struct. Fold Des. **8:**617–628.
29. **Lanman, J., T. T. Lam, S. Barnes, M. Sakalian, M. R. Emmett, A. G. Marshall, and P. E. Prevelige, Jr.** 2003. Identification of novel interactions in HIV-1 capsid protein assembly by high-resolution mass spectrometry. J. Mol. Biol. **325:**759–772.
30. **Le Blanc, I., M. C. Prevost, M. C. Dokhelar, and A. R. Rosenberg.** 2002. The PPPY motif of human T-cell leukemia virus type 1 Gag protein is required early in the budding process. J. Virol. **76:**10024–10029.
31. **Li, S., C. P. Hill, W. I. Sundquist, and J. T. Finch.** 2000. Image reconstructions of helical assemblies of the HIV-1 CA protein. Nature **407:**409–413.
32. **Lim, D., M. Orlova, and S. P. Goff.** 2002. Mutations of the RNase H C helix of the Moloney murine leukemia virus reverse transcriptase reveal defects in polypurine tract recognition. J. Virol. **76:**8360–8373.
33. **Mayo, K., D. Huseby, J. McDermott, B. Arvidson, L. Finlay, and E. Barklis.** 2003. Retrovirus capsid protein assembly arrangements. J. Mol. Biol. **325:**225–237.
34. **Mayo, K., M. L. Vana, J. McDermott, D. Huseby, J. Leis, and E. Barklis.** 2002. Analysis of Rous sarcoma virus capsid protein variants assembled on lipid monolayers. J. Mol. Biol. **316:**667–678.
35. **Mortuza, G. B., L. F. Haire, A. Stevens, S. J. Smerdon, J. P. Stoye, and I. A. Taylor.** 2004. High-resolution structure of a retroviral capsid hexameric amino-terminal domain. Nature **431:**481–485.
36. **Payne, G. S.** 1990. Genetic analysis of clathrin function in yeast. J. Membr. Biol **116:**93–105.

37. **Reicin, A. S., A. Ohagen, L. Yin, S. Hoglund, and S. P. Goff.** 1996. The role of Gag in human immunodeficiency virus type 1 virion morphogenesis and early steps of the viral life cycle. J. Virol. **70:**8645–8652.
38. **Rein, A., M. R. McClure, N. R. Rice, R. B. Luftig, and A. M. Schultz.** 1986. Myristylation site in Pr65gag is essential for virus particle formation by Moloney murine leukemia virus. Proc. Natl. Acad. Sci. USA **83:**7246–7250.
39. **Scholz, I., B. Arvidson, D. Huseby, and E. Barklis.** 2005. Virus particle core defects caused by mutations in the human immunodeficiency virus capsid N-terminal domain. J. Virol. **79:**1470–1479.
40. **Singh, I. R., R. A. Crowley, and P. O. Brown.** 1997. High-resolution functional mapping of a cloned gene by genetic footprinting. Proc. Natl. Acad. Sci. USA **94:**1304–1309.
41. **Strack, B., A. Calistri, S. Craig, E. Popova, and H. G. Gottlinger.** 2003. AIP1/ALIX is a binding partner for HIV-1 p6 and EIAV p9 functioning in virus budding. Cell **114:**689–699.
42. **Swanstrom, R., and J. W. Wills.** 1997. Synthesis, assembly, and processing of viral proteins, p. 263–334. *In* J. M. Coffin, S. H. Hughes, and H. E. Varmus (ed.), Retroviruses. Cold Spring Harbor Laboratory Press, Cold Spring Harbor, N.Y.
43. **Tang, S., T. Murakami, B. E. Agresta, S. Campbell, E. O. Freed, and J. G. Levin.** 2001. Human immunodeficiency virus type 1 N-terminal capsid mutants that exhibit aberrant core morphology and are blocked in initiation of reverse transcription in infected cells. J. Virol. **75:**9357–9366.
44. **Tang, S., T. Murakami, N. Cheng, A. C. Steven, E. O. Freed, and J. G. Levin.** 2003. Human immunodeficiency virus type 1 N-terminal capsid mutants containing cores with abnormally high levels of capsid protein and virtually no reverse transcriptase. J. Virol. **77:**12592–12602.
45. **Telesnitsky, A., S. Blain, and S. P. Goff.** 1995. Assays for retroviral reverse transcriptase. Methods Enzymol. **262:**347–362.
46. **von Schwedler, U. K., T. L. Stemmler, V. Y. Klishko, S. Li, K. H. Albertine, D. R. Davis, and W. I. Sundquist.** 1998. Proteolytic refolding of the HIV-1 capsid protein amino-terminus facilitates viral core assembly. EMBO J. **17:**1555–1568.
47. **von Schwedler, U. K., K. M. Stray, J. E. Garrus, and W. I. Sundquist.** 2003. Functional surfaces of the human immunodeficiency virus type 1 capsid protein. J. Virol. **77:**5439–5450.
48. **von Schwedler, U. K., M. Stuchell, B. Muller, D. M. Ward, H. Y. Chung, E. Morita, H. E. Wang, T. Davis, G. P. He, D. M. Cimbora, A. Scott, H. G. Krausslich, J. Kaplan, S. G. Morham, and W. I. Sundquist.** 2003. The protein network of HIV budding. Cell **114:**701–713.
49. **Wang, M. Q., W. Kim, G. Gao, T. A. Torrey, H. C. Morse III, P. De Camilli, and S. P. Goff.** 2003. Endophilins interact with Moloney murine leukemia virus Gag and modulate virion production. J. Biol. **3:**4.
50. **Wills, J. W., C. E. Cameron, C. B. Wilson, Y. Xiang, R. P. Bennett, and J. Leis.** 1994. An assembly domain of the Rous sarcoma virus Gag protein required late in budding. J. Virol. **68:**6605–6618.
51. **Yasuda, J., and E. Hunter.** 1998. A proline-rich motif (PPPY) in the Gag polyprotein of Mason-Pfizer monkey virus plays a maturation-independent role in virion release. J. Virol. **72:**4095–4103.
52. **Yeager, M., E. M. Wilson-Kubalek, S. G. Weiner, P. O. Brown, and A. Rein.** 1998. Supramolecular organization of immature and mature murine leukemia virus revealed by electron cryo-microscopy: implications for retroviral assembly mechanisms. Proc. Natl. Acad. Sci. USA **95:**7299–7304.
53. **Yuan, B., S. Campbell, E. Bacharach, A. Rein, and S. P. Goff.** 2000. Infectivity of Moloney murine leukemia virus defective in late assembly events is restored by late assembly domains of other retroviruses. J. Virol. **74:**7250–7260.
54. **Yuan, B., X. Li, and S. P. Goff.** 1999. Mutations altering the Moloney murine leukemia virus p12 Gag protein affect virion production and early events of the virus life cycle. EMBO J. **18:**4700–4710.